Bioprocess Biosyst Eng (2009) 32:485–492
DOI 10.1007/s00449-008-0268-7

ORIGINAL PAPER

Electrochemical nitrite biosensor based on the immobilization of hemoglobin on an electrode modified by multiwall carbon nanotubes and positively charged gold nanoparticle

Lingyan Zhang · Min Yi

Received: 4 February 2008 / Accepted: 26 September 2008 / Published online: 22 October 2008

Abstract The report is on an electrochemical biosensor with remarkably improved sensitivity toward nitrite. In this strategy, positively charged gold nanoparticle (PCNA) is used in combination with multiwall carbon nanotubes (MWCNT) by electrostatic adsorption for fabricating PCNA/MWCNT films. Then hemoglobin (Hb) biocatalyst will easily be attached to the surface of the combination films aforementioned. After that, the Hb/PCNA films are immobilized onto the Hb/PCNA/MWCNT films through layer-by-layer assembly technique. The $(Hb/PCNA)_2$/MWNT/GC electrode thus prepared exhibits enhanced electrocatalytic behavior to the reduction of nitrite at −0.10 V versus SCE in 0.05 M H_2SO_4 solution. On condition of the low detecting potential and low pH, interference caused by direct electrochemical oxidation or oxidizable substances can be prevented. Therefore, the modified electrode shows fast response time, very high sensitivity, good selectivity and stability. The current response of the sensor increases linearly with nitrite concentration from a range of 3.6×10^{-6} to 3.0×10^{-3} M with a detection limit($S/N = 3$) of 9.6×10^{-7} M.

L. Zhang (✉) · M. Yi
Forensic Identification Center, College of Criminal Investigation, Southwest University of Political Science and Law, 401120 Chongqing, China
e-mail: zly100@126.com; ct100@126.com

L. Zhang · M. Yi
Chongqing Institutions of Higher Learning Center of Forensic Science Engineering and Research, Forensic Identification Center, Southwest University of Political Science and Law, 401120 Chongqing, China

Keywords Positively charged gold nanoparticle · Multiwall carbon nanotubes · Electrocatalytic · Hemoglobin · Nitrite

Introduction

Nitrite, which is one of the most dangerous toxic substances in environmental processes, food supplies and forensic science, is generally regarded as potential carcinogenic in human body. Therefore, early detection of nitrite is important in protecting water resources and food supplies to prevent carcinogenesis. Common laboratory-based analytical methods for determining nitrite include UV-visible spectra [1] and ion chromatograph [2], which are reliable but time-consuming or complicated, etc. Thus the electrochemical sensors are receiving considerable attention because of quick response, low-cost, high sensitivity as well as the ability to be miniaturized. Electrochemical nitrite sensors commonly rely on monitoring the electrocatalytic current of modified electrode to nitrite. This is due to the fact that the applied potential of the reduction of nitrite is relatively lower compared to that of the nitrite oxidation, which tends to invite interference from coexisting substances [3]. Several reports have appeared on detection of nitrite by using electrochemical sensors, which include heteropolyanion-modified electrode [4], polyaniline/carbon nanotube composite modified electrode [3], carbon nanotubes (CNT) powder microelectrode [5], direct electrochemistry and electrocatalysis of hemoglobin in sodium alginate film on a $BMIMPF_6$ modified carbon paste electrode [6], hemoglobin/colloidal silver nanoparticles immobilized in titania sol–gel film on glassy carbon electrode: direct electrochemistry and electrocatalysis [7], direct electrochemistry and electrocatalysis of hybrid film

assembled by polyelectrolyte–surfactant polymer, carbon nanotubes and hemoglobin [8], direct electrochemistry of hemoglobin and its electrocatalytic effect based on its direct immobilization on carbon ionic liquid electrode [9] or direct electrochemistry and electrocatalysis of hemoglobin in gelatine film modified glassy carbon electrode [10].

Interest in metal nanoparticle films is stimulated from their technological importance, as they display unique optical properties, magnetic properties, electronic properties and a surface area three orders of magnitude greater than micro-scale material [11]. Although actual applications of such films have yet not been realized, metal nanoparticle films such as negatively charged gold nanoparticle (prepared in aqueous solutions) [12], positively charged gold nanoparticles (PCNA) [13, 14], Pd [15], Pt [16] and Ag [17] show promise in the development of novel electrical and optical sensors, as catalysts, and precursors for metallic films. In particular, due to the relatively simple preparation, negatively charged gold nanoparticle has been an intensive research subject for the design of sensors [18–20]. However, water-based syntheses of gold nanoparticle is fraught with problems as a result of ionic interactions, which are typically overcome by using low reactant concentrations [13, 14]. Compared to those nanoparticles prepared in aqueous solution, PCNA synthesized in organic solvents can be made at relatively high concentrations with predefined size and shape, with improved monodispersity [13, 14]. In addition, compared with negatively charged gold nanoparticle, PCNA is synthesized in toluene by using tetraoctylammonium salts as the stabilizing agent, has more efficient electrocatalytic catalysis [13, 14]. To our knowledge, so far the potential applications of PCNA are not studied sufficiently.

On the other hand, semiconductor nano-materials such as carbon nanotubes (CNT) [21, 22], SiO_2 [23], TiO_2 [24] and CdS [25] have been the subject of much research in recent years, primarily due to the interest in their chemical stability [26, 27], ballistic conduction properties and surface binding phenomenon [28, 29]. Such novel properties of semiconductor nanoparticles provide the potential for substantial improvements in chemical sensors, nanoscale electronic devices, electrode materials in batteries and field-effect transistors, etc. [30]. Particularly, both single-walled carbon nanotubes (SWCNT) and multi-walled carbon nanotubes (MWCNT) now emerge in sensors applications owing to the ability of CNT to promote the electron-transfer reactions of important biomolecules, including cytochrome *c* [31], ascorbic acid [32], H_2O_2 [18, 33] and tripropylamine [34].

Thus, it is suggested that the achieved faradic response of the Hb is due to the ability of MWCNT to promote the electron transfer of enzymes. And the Hb exhibits the features of an enzyme and acts in an electrocatalytic manner in the reduction of nitrite.

In order to optimize the use of CNT in various further applications, the research on the modification of CNT with metal nanoparticle has been widely reported [22, 35]. Although the functionalized CNT with metal nanoparticle exhibits more excellent electrochemical behavior toward biomolecules, and some investigations have been conducted for the fabrication of biosensors based on the functionalized CNT with metal nanoparticle. The report on the electrocatalytic reduction of nitrite at $(Hb/PCNA)_2$/WCNT-modified electrode has not been available so far. The objective of the present work is to study a new approach for the electroanalytical determination of nitrite at the $(Hb/PCNA)_2$/WCNT-modified electrode. It can be envisaged that direct adsorption of PCNA onto the WCNT surface by the electrostatic interaction would not destroy the sp^2 structures of WCNT rather than covalent modification of WCNT surface; and hence, preserve their mechanical and electronic properties [36]. Here, PCNA is used in combination with multiwall carbon nanotubes by electrostatic adsorption for fabricating the PCNA/MWCNT films. Then Hb biocatalyst will easily be attached to the surface of the combination films aforementioned. After that, the Hb/PCNA films are immobilized onto the Hb/PCNA/MWCNT films through layer-by-layer assembly technique. The $(Hb/PCNA)_2$/MWNT/GC electrode thus prepared responds more sensitively to nitrite (even without the aid of an electron mediator) than those modified by the Hb/PCNA/WCNT, the PCNA/WCNT or the WCNT alone. Moreover, the $(Hb/PCNA)_2$/MWNT/GC electrode displays a higher active, fast, selective and stable features. The properties of the functional WCNT films, combined with the electrocatalytic activity, could make them useful for the investigation of protein electrochemistry and the development of bioelectronic devices at functional interface.

Experimental section

Experimental setup

The MWCNT are dispersed, as suggested by transmission electron microscopy (TEM) data using TECNAI 10 (PHILIPS FEI Co., Holland). Raman spectras of the films were obtained with Raman spectral comparator (Foram 685-2. Foster and Freeman Ltd). The scan electron microscopy (SEM) images of the films were performed on scanning probe microscope (SMP) (Vecco, USA) and FEI Nova 400 FEG-Sem (FEI, USA). Amperometric experiments were performed by using a CHI 660C electrochemical work station (Shanghai CH Instruments Co., China) in a three-electrode electrochemical cell. A modified GC electrode

(Φ = 4 mm) is served as a working electrode with a platinum wire auxiliary electrode and a saturated calomel electrode (SCE) reference electrode. Moreover, the amperometric experiments were performed in 0.05 M H_2SO_4, which were deoxygenated with highly pure nitrogen for 30 min before electrochemical experiments and a nitrogen atmosphere was kept over the solution during measurements.

Materials

MWCNT (MWNT, >95% purity) was purchased from Chengdu Organic Chemicals Co., Ltd., Chinese Academy of Sciences. Prior to use, MWNT were treated with concentrated nitric acid in order to introduce carboxylic acid groups according to the report [37]. Bovine (horse heart) hemoglobin (Hb) was purchased from Sigma Chemical Co., (St. Louis, MO, USA). $NaNO_2$, H_2SO_4 and all other chemicals were obtained from Chemical Reagent Company, Sichuan, China.

The details of the synthesis processes of PCNA are described in the previous reports [13, 14]: A 30-mM aqueous metal chloride solution was added to a solution of tetraoctylammonium bromide in toluene. Then a solution of freshly prepared $NaBH_4$ was added to the stirred mixture. After the two phases were separated. The toluene phase was subsequently washed with 0.1 M H_2SO_4, 0.1 M NaOH and H_2O_2, respectively. After that, the toluene phase dried over anhydrous Na_2SO_4. Direct phase transfer across the organic/aqueous boundary: 0.1 M 4-dimethylaminopyridine solution of the as prepared nanoparticle mixtures, which was added to the toluene phase. Then, nanoparticles from larger volumes of the toluene phase have also been successfully transferred into water. TEM analysis indicates that the PCNA is ~10 nm (Fig. 1a).

Electrodes preparation

Because carbon nanotubes are very hydrophobic, most metal nanoparticles cannot adhere to carbon nanotubes and physical adsorbed metal nanoparticles can be easily removed by agitating the material in liquid by agglomeration [38, 39]. Electroless deposition method, electrostatic adsorption or chemical reaction with MWCNT have thus been suggested to improve metal deposition onto carbon nanotubes [22, 40]. Our strategy for the immobilization of positively charged metal nanoparticle layers on MWCNT surfaces is convenient and effective. Therefore the fabrication of the nitrite electrode is as below:

First, sodium dodecyl sulfate (SDS) was used to solubilize and disperse MWCNT according to the literature [41]. One milligram of the acid-treated MWCNT (functionalizing with carboxylic acid groups) was dispersed in 1 mL of 1.5 mg/mL sodium dodecyl sulfate to give a 1 mg/mL MWCNT black suspension with the aid of ultrasonic agitation (Fig. 1b). A total of 10 μL MWCNT suspension was cast on a cleaned GC electrode surface to form a stable MWCNT film with abundant negative charge. The MWNT-modified electrode (MWNT/GC) was then allowed to air dry [41]. Subsequently, the MWNT/GC electrode was immersed into PCNA solution for 4 h. Then it was possible to merge PCNA on the MWCNT-modified electrode via oppositely charged adsorption, which was characterized by TEM in Fig. 1c. After that, Hb was assembled onto the PCNA/MWNT/GC electrode by immersing the PCNA/MWNT/GC electrode in 10 mg/mL Hb solution for 4 h. Eventually, the $(Hb/PCNA)_2$/MWNT/GC electrode was constructed by alternately immersing the Hb/PCNA/MWNT/GC electrode into PCNA and 10 mg/mL Hb solution for 4 h each with intermediate water-washing. Then, the $(Hb/PCNA)_2$/MWNT/GC electrode was kept at 4 °C until it was used.

Results and discussion

Characteristics of the $(Hb/PCNA)_2$/MWNT/GC electrode

Experiment cyclic voltammograms in 0.05 M H_2SO_4 are plotted in Fig. 2. MWNT/GC electrode displays two reduction peaks and one oxidation peak in the range of the

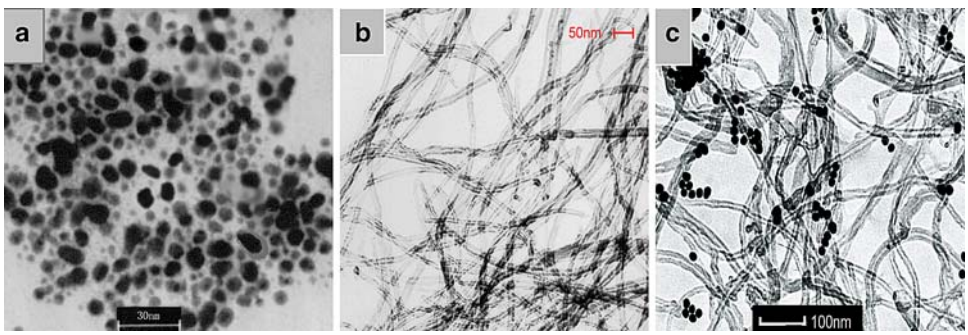

Fig. 1 TEM images of positively charged nano-Au film (**a**), MWCNT film (**b**), and PCNA/MWCNT films (**c**)

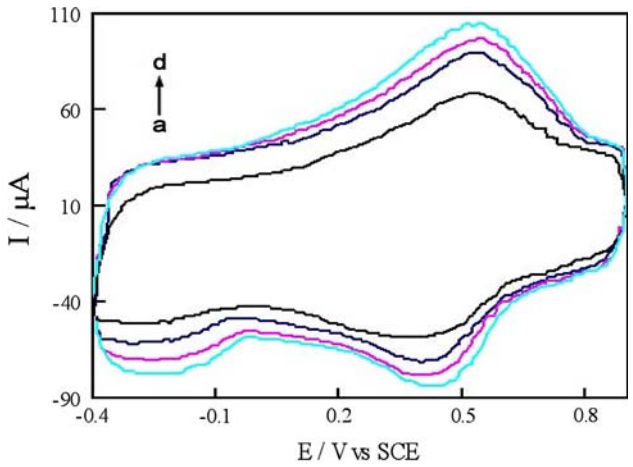

Fig. 2 CVs of MWCNT-modified electrode (*a*), PCNA/MWCNT-modified electrode (*b*), $(Hb/PCNA)_2$/MWCNT T-modified electrode (*c*), and Hb/PCNA/MWCN-modified electrode (*d*) at scan rate of 100 mV/s in 0.05 M H_2SO_4

voltage between −0.4 and 0.8 V (Fig. 2a) because of the specific electrochemical properties of MWNT [41]. Comparing the results of Fig. 2b (PCNA/MWCNT-modified electrode) with Fig. 2a, the peak currents have increased. It can be ascribed to the presence of PCNA, which as electron antennae could efficiently tunnel electrons between the electrode and the electrolyte. When Hb is entrapped on the PCNA/MWCNT-modified electrode, a more obvious reduction/oxidation peak is observed in Fig. 2d. This is due to the fact that MWNT can facilitate fast direct electron transfer between redox proteins and electrode surface [42–44]. In the following procedures, Hb/PCNA is assembled on the Hb/PCNA/MWCNT-modified electrode, the CVs of $(Hb/PCNA)_2$/MWCNT-modified electrode is reduced (Fig. 2c). The reasonable explanation for why the transfer of the electron to the electrode surface becomes more difficult may be due to the increase in the quantity of Hb assembled onto the electrode. The CVs of modification process shows that the $(Hb/PCNA)_2$ films can be immobilized on the MWNT film based on the layer-by-layer assembly technique. Moreover, the CVs of the $(Hb/PCNA)_2$/MWCNT-modified electrode at different scan rates have been studied. It is found that both the anodic and cathodic peak currents increase linearly with scan rate from 0.01 to 0.14 V/s, which indicates a surface-controlled process.

SEM is a powerful tool for studying the surface morphologies of the membranes. The morphology of the MWCNT film (Fig. 3a) shows a network-like structure. Compared with the MWCNT film, the SEM image of PCNA/MWCNT films (Fig. 3b) has obviously changed, on which the light dot is observable due to the assembly of PCNA. More coral-shaped particles are distributed uniformly on the surface while Hb is presented on the PCNA/MWCNT films (Fig. 3c).

On the other hand, Raman spectra of MWCNT, PCNA/MWCNT, and Hb/PCNA/MWCNT film are shown in Fig. 4. The MWCNT film (Fig. 4a) shows a disorder-induced peak around 1,350 cm^{-1}, which is similar to that obtained by Shift et al. [45]. The reason may correspond to the D-lind associated with disorder-allowed zone-edge modes of graphite [45]. When PCNA is self-assembled on MWCNT film by electrostatic interactions, a significant increase of the intensity of D-band and G-band (Fig. 4c) can be observed in Raman spectra, owing to the unique optical property of PCNA. After Hb is coated on the PCNA/MWCNT films, the peak value of the Hb/PCNA/MWCNT films diminish drastically as shown in Fig. 4b.

Electrocatalytic activity of the $(Hb/PCNA)_2$/MWNT/GC electrode

To confirm the electrocatalytic activity of the $(Hb/PCNA)_2$/MWCNT-modified electrode toward nitrite, an experiment is performed in 0.05 M H_2SO_4 containing nitrite with different concentrations. With the addition of nitrite, obviously enhanced cathodic peak current are observed (Fig. 5b, c, d,); increasing the nitrite concentrations (0, 3.3×10^{-3}, 5.0×10^{-3} M) resulted in dramatic increase of reduction peak current of the modified electrode. These results indicate that $(Hb/PCNA)_2$/MWCNT-modified electrode exhibits excellent electroactivity toward nitrite. The mechanism of NO_2^- reduction at the $(Hb/PCNA)_2$/MWNT film is yet not clear, but probably similar to that reported by Yao [3] and Lu[8]:

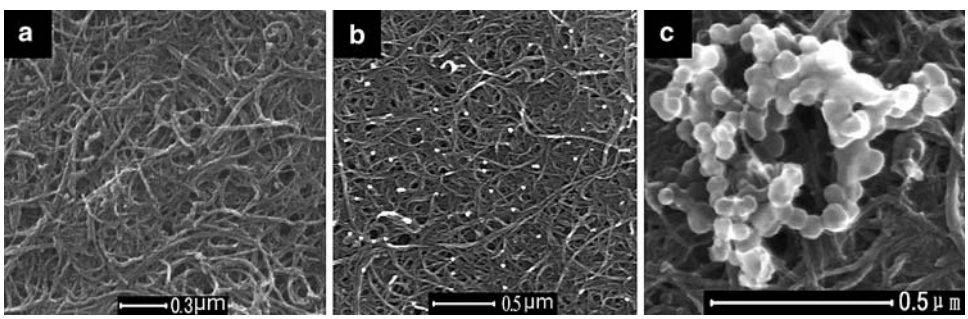

Fig. 3 SEM images of MWCNT film (**a**), PCNA/MWCNT films (**b**), and Hb/PCNA/MWCNT films (**c**)

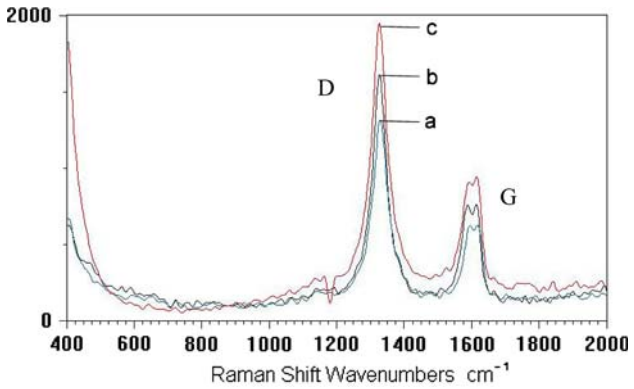

Fig. 4 Raman images of MWCNT film (*a*), Hb/PCNA/MWCNT films (*b*), and PCNA/MWCNT films (*c*)

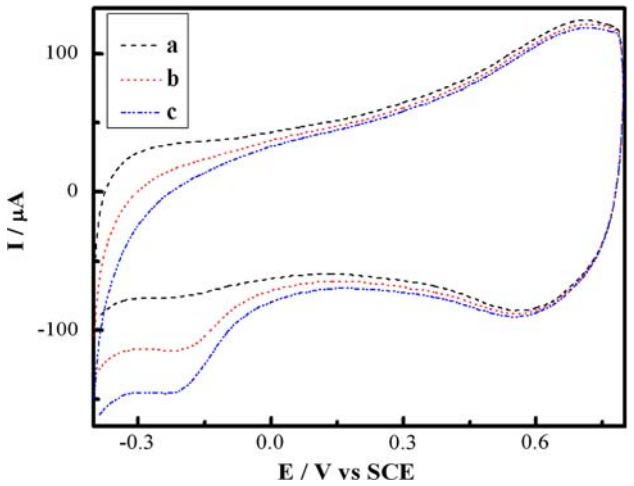

Fig. 5 CVs of $(Hb/PCNA)_2$/MWCNT-modified electrode at scan rate of 100 mV/s in 0.05 M H_2SO_4 without nitrite (*a*), with 3.3×10^{-3} M (*b*) and 5.0×10^{-3} M nitrite (*c*)

$$2NO_2^- + 2H^+ + HbHFe(II) \rightarrow HbHFe(III) + 2NO + 2H_2O$$

Estimation of the biosensor construction

Using Hb for practical applications requires that it is active, stable and kept at high concentration in close vicinity of the electrode surface [46]. Thus, six different strategies for the preparation of nitrite biosensors are compared at −0.10 V in 0.05 M H_2SO_4. Figure 6 shows the comparison of the amperometric responses of a Hb/GC electrode (Fig. 6a), MWCNT/GC electrode (Fig. 6b), PCNA/MWCNT/GC electrode (Fig. 6c), Hb/MWCNT/GC electrode (Fig. 6d), Hb/PCNA/MWCNT/GC electrode (Fig. 6e) and $(Hb/PCNA)_2$/MWCNT/GC electrode (Fig. 6f) to successive additions of different concentrations nitrite, respectively. Compared with the Hb/GC electrode (Fig. 6a), the MWCNT-modified electrode (Fig. 6b) exhibits higher

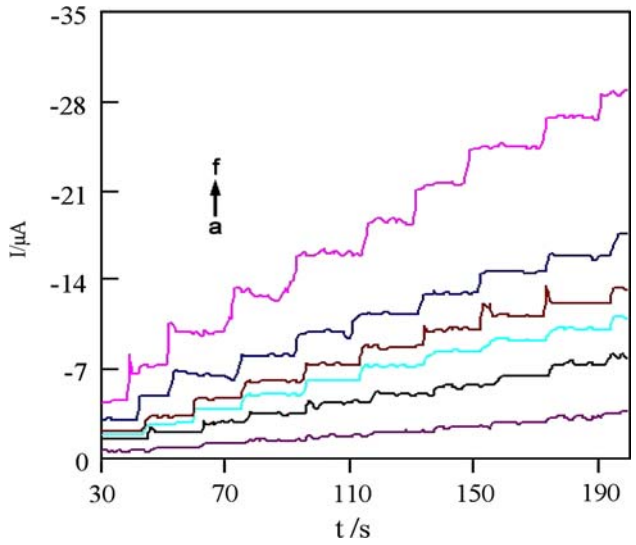

Fig. 6 Amperometric current-time curves at constant potential of −0.10 V in 0.05 M H_2SO_4 with successive addition of 0.2 mM nitrite for: Hb-modified electrode (*a*), MWNT-modified electrode (*b*), PCNA/MWNT-modified electrode (*c*), Hb/MWNT-modified electrode (*d*), Hb/PCNA/MWNT-modified electrode (*e*), and $(Hb/PCNA)_2$/MWCNT-modified electrode (*f*)

electroactivity toward nitrite. It is due to the fact that Hb cannot adhere to the GC electrode and physical adsorbed Hb can be easily removed by agitating in liquid. Hence, the Hb/GC electrode exhibits lower electroactivity toward nitrite. However, the PCNA/MWCNT-modified electrode (Fig. 6c) exhibits higher electroactivity toward nitrite than that of the MWCNT-modified electrode. This improved analytical performance is attributed to PCNA. PCNA, which is synthesized in toluene by using tetraoctylammonium salts as the stabilizing agent, can be made at relatively high concentrations with improved monodispersity, predefined size and predefined shape [13, 14]. Therefore, PCNA has more efficient electrocatalytic catalysis [13, 14]. As is expected, since MWNT has the ability to facilitate or promote the electron transfer between proteins and electrode, a higher current response for nitrite determination is achieved by using the Hb/MWCNT/GC electrode (Fig. 6d) when compared with the current response values at the PCNA/MWCNT-modified electrode. In this experiment, the largest current response is obtained from the $(Hb/PCNA)_2$/MWCNT-modified electrode (Fig. 6f). However, no obvious increase in the current response is observed at the $(Hb/PCNA)_3$/MWCNT-modified electrode as compared with the $(Hb/PCNA)_2$/MWCNT-modified electrode, which suggests the quality of Hb has reached a saturation for the $(Hb/PCNA)_2$/MWCNT-modified electrode. In order to achieve the largest possible sensitivity, the $(Hb/PCNA)_2$/MWCNT-modified electrode is selected to fabricate the nitrite sensor. Moreover, the

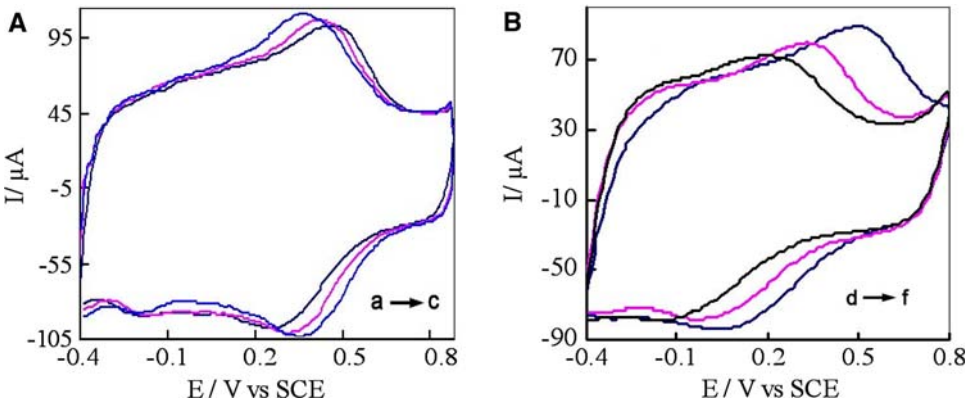

Fig. 7 CVs of $(Hb/PCNA)_2$/MWCNT-modified electrode in H_2SO_4 (**A**) or PBS (**B**) at various pH values in the absence of nitrite: 0.05 M H_2SO_4 (*a*); 0.1 M H_2SO_4 (*b*); 0.5 M H_2SO_4 (*c*); pH 5.00 (*d*); pH 4.50 (*e*); and pH 4.00 (*f*). Scan rate, 100 mV/s

response times are similar among the six designs, with the steady-state current being reached in a few seconds.

Optimization of supporting electrolyte

The influence of the acidity of the supporting electrolyte on the current response is investigated to evaluate the best performance of the sensor. Figure 7 shows the CVs of the $(Hb/PCNA)_2$/MWCNT/GC electrode in H_2SO_4 or PBS in absence of nitrite. It is found that both the cathodic (E_{pc}) and the anodic (E_{pa}) potential of the modified electrode positively shift with the H_2SO_4 concentration in the range from 0.05 M to 0.5 M (Fig. 7A). In contrast, both the cathodic (E_{pc}) and the anodic (E_{pa}) potential of the modified electrode negatively shift with the increase in pH (Fig. 7B).

Moreover, the current responses of the $(Hb/PCNA)_2$/MWCNT-modified electrode to nitrite are measured in PBS or H_2SO_4 with a scan rate 100 mV s^{-1}. The electrode exhibits lower electrocatalytic activity for nitrite in PBS of varying pH. Surprisingly, comparing with the electrode in PBS, the electrode offers a dramatic enhancement of the sensitivity in H_2SO_4, and the electrode shows the highest sensitivity toward nitrite in 0.1 M H_2SO_4 (Fig. 8a) than that of the electrode in 0.05 M H_2SO_4 (Fig. 8b), 0.5 M H_2SO_4 (Fig. 8c) and 1.0 M H_2SO_4 (Fig. 8d). Considering the effects of the response sensitivity as well as the denaturation of the Hb, 0.05 M H_2SO_4 is chosen for the subsequent experiments.

Calibration curve of standard nitrite solutions

Figure 9 shows a calibration plot for consecutive additions of aliquots of a nitrite solution in 0.05 M H_2SO_4 at room temperature. The catalytic current of the modified electrode increases linearly with the nitrite concentration in the range from 3.6×10^{-6} to 3.0×10^{-3} M with a detection limit ($S/N = 3$) of 9.6×10^{-7} M. The linear regression equation is i (μA) = $3.3263 \pm 1.5338[NO_2^-]$ (mM) with a correlation coefficient of 0.997. The modified electrode shows

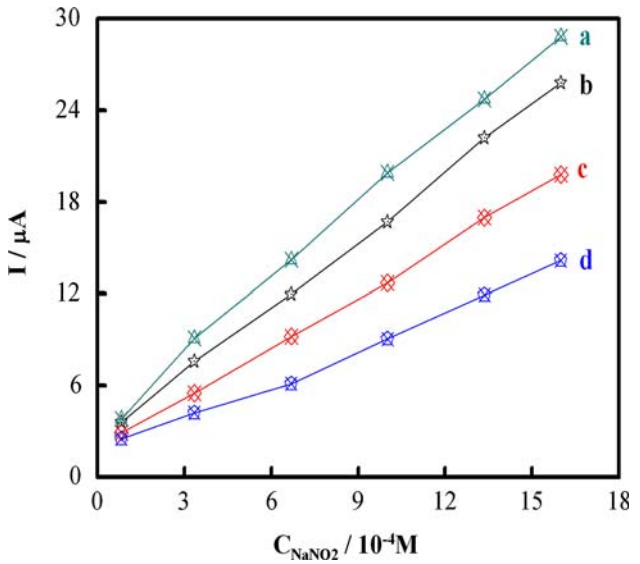

Fig. 8 Calibration curve of the current response of $(Hb/PCNA)_2$/MWCNT-modified electrode to nitrite in different H_2SO_4: 0.1 M H_2SO_4 (*a*); 0.05 M H_2SO_4 (*b*); 0.5 M H_2SO_4 (*c*) and1.0 M H_2SO_4 (*d*)

higher sensitivity and lower detection limit than any other reported papers in the acid medium [3, 6–9].

When the concentration of nitrite is higher than 3.0×10^{-3} M, the calibration curve tends to level off, thus, it shows the characteristics of the Michaelis–Menten kinetic mechanism. The apparent Michaelis–Menten constant (K_M^{app}), which gives an indication of the enzyme–substrate kinetics, can be obtained from the electrochemical version of the Lineweaver–Burk equation [8]:

$$1/I_{SS} = 1/I_{max} + K_M^{app}/I_{max}C$$

Here I_{SS} is the steady-state current after the addition of substrate. I_{max} is the maximum current under saturated substrate condition and C is the bulk concentrate of the substrate. The K_M^{app} value for the $(Hb/PCNA)_2$/MWCNT/GC electrode is estimated to be 6.2×10^{-4} M. The low value of K_M^{app} indicates that Hb immobilized in Hb/

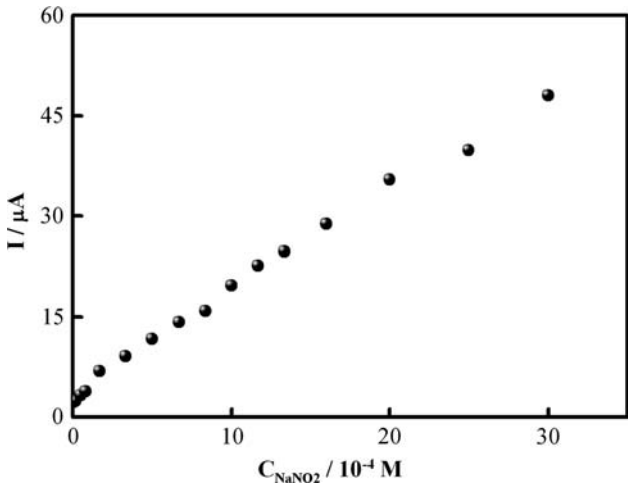

Fig. 9 Calibration curve of $(Hb/PCNA)_2$/MWCNT-modified electrode to nitrite determination in 0.05 M H_2SO_4 at an applied potential of −0.10 V

$PCNA)_2$/MWCNT film retains a high biological affinity to nitrite.

Selectivity and stability study

Interference experiment for the detection of nitrite at the modified electrode is investigated by comparing with the current response before and after the addition of some possible interferents into the 0.05 M H_2SO_4 containing 0.4 mM nitrite. Possible interference such as hydrogen peroxide, milk, ascorbic acid and uric acid in the same concentration of nitrite had no obviously effect on the detection. Moreover, the common ions such as 0.4 mM Na^+, K^+, HPO_4^{2-}, $H_2PO_4^{2-}$, Cl^- and Ca^{2+} do not show interference to the determination of nitrite. The mechanism is yet not clear, but probable due to the low detecting potential and low pH, interference caused by direct electrochemical oxidation or oxidizable substances can be prevented at the modified electrode. It indicated that this protocol is of high selectivity.

Stability studies of continuous cyclic scans on the $(Hb/PCNA)_2$/MWCNT-modified electrode are carried out in 0.05 M H_2SO_4 without nitrite. Then, the electrocatalytic activities of the $(Hb/PCNA)_2$/MWCNT-modified electrode toward nitrite are measured in 0.05 M H_2SO_4 by chronoamperometry, and record the chronoamperometry responses. After that, the two experiments mentioned above are performed again. The amperometric response of the electrode decrease to 93.6, 90.9 and 84.8% of the initial response in the 100, 200 and 400 continuous cycles, respectively. Surprisingly, hound little change in electrocatalytic activities of the same electrode toward nitrite after 100, 200 and 400 continuous cycles, respectively.

On the other hand, the storage stability of the proposed biosensor is studied after the modified electrode is suspended above phosphate buffer at 4 °C in a refrigerator for 30 days. The cyclic voltammograms response of the electrode decrease to 88.8% of the initial response. These results prove that the $(Hb/PCNA)_2$/MWCNT-modified electrode is of high good stabilities.

Conclusion

In this experiment, we have demonstrated the use of $(Hb/PCNA)_2$/MWCNT-modified electrode for a greatly enhanced amperometric biosensor of nitrite in 0.05 M H_2SO_4. Due to the low detecting potential and low pH, interference caused by direct electrochemical oxidation or oxidizable substances can be prevented at the modified electrode. Furthermore, the modified electrode shows high stability and good repeatability. This method offers an economical, simple, and convenient way to obtain high-quality detectors for the detection of nitrite.

Acknowledgments This work has been supported by the Education Committee Foundation of Chongqing City, China (KJ070104), the Education Committee Foundation of Chongqing City, China (KJ070103), the Moe Key Luminescence and Real-Time Analysis, Chongqing (CSTC,2006CA8006).

References

1. Xu X, Ying XH, Duan BW (2007) Determination of nitrite and nitrate in pickled vegetables by ion chromatography with ultraviolet detection. Food Ferment Ind (in Chinese) 33:120–122
2. Wang XY, Xiang XH, Tu XM, Kang JX (2002) Determination of the residual nitrate/nitrite in foods by UV detection-ion chromatography. Chem Anal Meter (in Chinese) 1128–1129
3. Guo ML, Chen JH, Li J, Tao B, Yao SZ (2005) Fabrication of polyaniline of carbon nanotube composite modified electrode and its electrocatalytic property to the reduction of nitrite. Anal Chim Acta Anal Chim Acta 532:71–77
4. Wang Sf, Du D (2003) Preparation and electrochemical properties of Keggin-type phosphomolybdic anions in electrostatically linked L-cysteine self-assembled monolayers. Sens Actuators B 94:282–289
5. Zhao YD, Zhang WD, Luo QM, Li SFY (2003) The oxidation and reduction behavior of nitrite at carbon nanotube powder microelectrodes. Microchem J 75:189–198
6. Wei S, Wang DD, Gao RF, Jiao K (2007) Direct electrochemistry and electrocatalysis of hemoglobin in sodium alginate film on a $BMIMPF_6$ modified carbon paste electrode. Electrochem Commun 9:1159–1164
7. Zhao S, Zhang K, Sun YY, Sun CQ (2006) Hemoglobin/colloidal silver nanoparticles immobilized in titania sol–gel film on glassy carbon electrode: direct electrochemistry and electrocatalysis. Bioelectrochemistry 69:10–15
8. Chen L, Lu GX (2006) Direct electrochemistry and electrocatalysis of hybrid film assembled by polyelectrolyte–surfactant polymer, carbon nanotubes and hemoglobin. J of Electroanal Chem 597:51–59

9. Safavi A, Maleki N, Moradlou O, Sorouri M (2008) Direct electrochemistry of hemoglobin and its electrocatalytic effect based on its direct immobilization on carbon ionic liquid electrode. Electrochem Commun 10:420–423
10. Yao H, Li N, Xu JZ, Zhu JJ (2007) Direct electrochemistry and electrocatalysis of hemoglobin in gelatine film modified glassy carbon electrode. Talanta 71:550–554
11. Lai J, Shafi KVPM, Ulman A, Loos K, Popovitz-Biro R, Lee Y, Vogt T, Estourmes C (2005) One-step synthesis of core(Cr)/shell(r-Fe_2O_3) nanoparticles. J Am Chem Soc 127:5730–5731
12. Zhang LY, Yuan R, Huang XQ, Chai YQ, Cao SR (2004) Potentiometric immunosensor based on antiserum of Japanese B encephalitis immobilized in nano-Au/polymerized *o*-phenylenediamine film. Electrochem Commun 6:1222–1226
13. Gittins DI, Caruso F (2001) Spontaneous phase transfer of nanoparticulate metals from organic to aqueous media. Angew Chem Int Ed 40:3001–3004
14. Zhang LY, Yuan R, Chai YQ, Li XL (2007) Investigation of the electrochemical and electrocatalytic behavior of positively charged gold nanoparticle and L-cysteine film on an Au electrode. Anal Chim Acta 596:99–105
15. Lim SH, Wei J, Lin JY, Li QT, You JK (2005) Glucose biosensor based on electrodeposition of palladium nanoparticles and glucose oxidase onto Nafion-solubilized carbon nanotube electrode. Biosens Bioelectron 20:2341–2346
16. Yu RQ, Chen LW, Liu QP, Lin JY, Tan K-L, Ng SC, Chan Hardy SO, Xu G-Q, Andy Hor TS (1998) Platinum deposition on carbon nanotubes via chemical modification. Chem Mater 10:718–722
17. Guo DJ, Li HL (2005) Highly dispersed Ag nanoparticles on functional MWNT surfaces for methanol oxidation in alkaline solution. Carbon 43:1259–1264
18. Yuan R, Zhang LY, Chai YQ, Li QF, Cao SR (2005) A label-free amperometric immunosensor based on multi-layer assembly of polymerized *o*-phenylenediamine B encephalitis vaccine. Anal Chim Acta 531:1–5
19. Zhang LY, Yuan R, Huang XQ, Chai YQ, Cao SR (2005) A new label-free amperometric immunosenor for rubella vaccine. Anal Bioanal Chem 381:1036–1040
20. Zhang LY, Yuan R, Chai YQ, Chen SH, Wang N (2006) Layer-by-layer self-assembly of films of nano-Au and $Co(bpy)_3$3+ for the determination of Japanese B encephalitis vaccine. Biochem Eng J 28:231–236
21. Wang J, Musameh M, Lin Y (2003) Solubilization of carbon nanotubes by nation toward the preparation of amperometric biosensors. J Am Chem Soc 125:2408–2409
22. Hrapovuc S, Liu Y, Male KB, Luong JHT (2004) Electrochemical biosensing platforms using platinum nanoparticles and carbon nanotubes. Anal Chem 76:1083–1088
23. Chen ZG, Tang DY (2007) Antigen–antibody interaction from quartz crystal microbalance immunosensors based on magnetic $CoFe_2O_4/SiO_2$ composite nanoparticle-functionalized biomimetic interface. Bioprocess Biosys Eng 30:243–249
24. Kim BH, Ok SH, Cho DL, Lim SH, Yoo SY, KooK JK, Cho YI, Ohk SH, Ko YM (2007) Sterilization effects of a TiO_2 photocatalytic film against a *Streptococcus mutans* culture. Bioprocess Biosys Eng 12: 136–139
25. Shi JH, Qin YJ, Wu W, Li XL, Guo ZX, Zhu DB (2004) In situ synthesis of CdS nanoparticles on multi-walled carbon nanotubes. Carbon 42:455–458
26. Reddy ALM, Rajalakshmi N, Ramaprabhu S (2008) Gobalt-polyprrole-multiwalled carbon nanotube catalysts for hydrogen and alcohol fuel cells. Carbon 46:2–11
27. Padigi SK, Reddy RKK, Prasad S (2007) Carbon nanotube based aliphatic hydrocarbon sensor. Biosens Bioelectron 22:829–837
28. Lin Y, Taylor S, Li H, Fernando KAS, Qu L, Wang W, Gu L, Zhou S, Sun YP (2004) Advances toward bioapplications of carbon nanotubes. J Mater Chem 14:527–541
29. Sotiropoulou S, Chaniotakis NA (2003) Carbon nanotube array-based biosensor. Anal Bioanal Chem 375:103–105
30. Shim M, Javey A, Kam NWS, Dai H (2001) Polymer functionalization for air-stable n-type carbon nanotube field-effect transistors. J Am Chem Soc 123:11512–11513
31. Wang J, Li M, Shi Z, Gu N (2002) Direct electrochemistry of cytochrome *c* at a glassy carbon electrode modified with single-wall carbon nanotube. Anal Chem 74:1993–1997
32. Wang ZH, Liu MJ, Liang Q, Wang Y, Luo G (2002) Carbon nanotube-modified electrodes for the simultaneous determination of dopamine and ascorbic acid. Analyst 127:653–658
33. Luo XL, Killard Anthony J, Morrin A, Smyth MR (2006) Enhancement of a conducting polymer-based biosensor using carbon nanotube-doped polyaniline. Anal Chim Acta 575:39–44
34. Choi HN, Lee JY, Lyu YK, Lee W-Y (2006) Tris(2, 2′-bipyridyl)ruthenium(II) electrogenerated chemiluminescence sensor based on carbon nanotube dispersed in sol–gel-derived titania–Nafion composite films. Anal Chim Acta 565:48–55
35. Kim B, Sigmund W (2004) Functionalized multiwall carbon nanotube/gold nanoparticle composites. Langmuir 20:8239–8242
36. Lawrenc NS, Wang J (2006) Chemical adsorption of phenothiazine dyes onto carbon nanotubes: toward the low potential detection of NADH. Electrochem Commun 8:71–76
37. Guo ML, Chen JH, Nie LH, Yao SZ (2004) Electrostatic assembly of calf thymus DNA on multi-walled carbon nanotube modified gold electrode and its interaction with chlorpromazine hydrochloride. Electrochim Acta 49:2637–2643
38. Dujardin E, Ebbesen TW, Hiura H, Tanigaki K (1994) Capillarity and wetting of carbon nanotubes. Science 265:1850–1851
39. Lordi V, Yao N, Wei J (2001) Method for supporting platinum on single-walled carbon nanotubes for a selective hydrogenation catalyst. Chem Mater 13:733–737
40. Kong J, Chapline MG, Dai HJ (2001) Full and modulated chemical gating of individual carbon nanotubes by organic amine compounds. J Phys Chem 13:1384–2893
41. Zhang LY, Yuan R, Chai YQ, Cao SR, Li XL, Wang N (2006) Study on a hydrogen peroxide sensor based on horseradish peroxidase/nano-Au/horseradish peroxidase/multi-walled carbon nanotubes (in Chinese). Acta Chim Sinica 64:1711–1715
42. Gu HY, Yu AM, Chen HY (2001) Direct electron transfer and characterization of hemoglobin immobilized on a Au colloid–cysteamine-modified gold electrode. J Electroanal Chem 516: 119–126
43. Zhang JD, Oyama MJ (2005) Gold nanoparticle-attached ITO as a biocompatible matrix for myoglobin immobilization: direct electrochemistry and catalysis to hydrogen peroxide. Electroanal Chem 577:273–279
44. Liu SQ, Ju HX (2002) Renewable reagentless hydrogen peroxide sensor based on direct electron transfer of horseradish peroxidase immobilized on colloidal gold-modified electrode. Anal Biochem 307:110–116
45. Chen CC, Chen CF, Chen CM, Chuang FT (2007) Modification of multi-walled carbon nanotubes by microwave digestion method as electrocatalyst supports for direct methanol fuel cell applications. Electrochem Commun 9:159–163
46. Stolarczyk K, Nazaruk E, Rogalski J, Bilewicz R (2007) Mediatorless catalytic oxygen reduction at boron-doped diamond electrodes. Electrochem Commun 9:115–118